

Supporting Information for

Potential-Independent Intracellular Drug Delivery and Mitochondrial Targeting

Yin Liu^{1,2}, Jian Zhang¹, Ying Tu¹ and Lin Zhu^{1,*}

¹ Department of Pharmaceutical Sciences, Irma Lerma Rangel College of Pharmacy, Texas A&M University, College Station, Texas 77843, USA

² School of Environment, Hangzhou Institute for Advanced Study, UCAS, Hangzhou, Zhejiang Province 330106, China

* Corresponding author:

Lin Zhu, Ph.D.

Associate Professor, Department of Pharmaceutical Sciences, Irma Lerma Rangel College of Pharmacy, Texas A&M University

1010 West Ave. B, MSC 131,

Kingsville, Texas 78363, USA

Phone: (361)221-0757

Fax: (361)221-0793

Email: lzhu@tamu.edu

The SI file includes:

Supplementary text

Figures S1 to S28

Legend for Movie S1

SI References

Other supplementary materials for this manuscript include the following:

Movie S1

Supplementary Text

Materials and Methods

Materials. Methoxy polyethylene glycol maleimide (PEGm-MAL, m=1k, 2k and 5k Da), 1,2-distearoyl-sn-glycero-3-phosphoethanolamine N-[amino (polyethylene glycol)] (PEGm-PE, m=1k, 2k and 5k Da), and maleimide-polyethylene glycol (2k Da)-succinimidyl valerate (MAL-PEG2k-SVA) were purchased from Laysan Bio, Inc. (Arab, AL, USA). Pentafluoropropionic acid (F5-COOH), heptafluorobutyric acid (F7-COOH), perfluoropentanoic acid (F9-COOH), heptafluorobutyric anhydride were purchased from Matrix Scientific Co. (Columbia, SC, USA). 1H, 1H-Heptafluorobutylamine (F7-NH₂) and pentafluoropropionic anhydride were purchased from TCI America (Boston, MA, USA). 1,2-Dioleoyl-sn-glycero-3-phosphoethanolamine (DOPE), 1,2-dipalmitoyl-sn-glycero-3-phosphocholine (DPPC), 1,2-dipalmitoyl-sn-glycero-3-phospho-L-serine (sodium salt, DPPS), 1,2-dipalmitoyl-sn-glycero-3-phospho-(1'-rac-glycerol) (sodium salt, DPPG), 1,2-dioleoyl-3-trimethylammonium-propane (chloride salt, DOTAP), cardiolipin (sodium salt), and 1,2-dioleoyl-sn-glycero-3-phosphoethanolamine-N-(lissamine rhodamine B sulfonyl) (Rh-PE) were purchased from Avanti Polar Lipids, Inc. (Alabaster, AL, USA). TLC plates (silica gel 60 F254) were purchased from EMD Biosciences (La Jolla, CA, USA). N-Hydroxysuccinimide (NHS), 2',7' -dichlorodihydrofluorescein diacetate (H₂DCFDA), chlorpromazine hydrochloride, nystatin, pyrene, collagenase D, and 1-(3-dimethylaminopropyl)-3-ethylcarbodiimide hydrochloride (EDC·HCl) were purchased from Sigma-Aldrich Chemicals (St. Louis, MO, USA). L-cysteine ethyl ester hydrochloride, triethylamine (TEA), cholesterol, trifluoroacetic anhydride, and 2-hydroxypropyl-β-cyclodextrin (HP-β-CD) were obtained from Alfa Aesar (Haverhill, MA, USA). 3,3'-dioctadecyloxacarbocyanine perchlorate (DiO), 1,1'-dioctadecyl-3,3',3'-tetramethylindocarbocyanine perchlorate (DiI), fluorescein isothiocyanate (FITC), rhodamine123 (Rh123), chloroform, dichloromethane (DCM), dimethylformamide (DMF), methanol, ethyl acetate, hexane, ER-Tracker™ Green, and Mitochondria Isolation Kit for Cultured Cells were purchased from Thermo Fisher Scientific (Rockford, IL, USA). α-Vitamin E succinate (VES) was purchased from Spectrum Chemical Manufacturing Corp. (New Brunswick, NJ, USA). MitoView™ Green, MitoView™ 633, NBD C6-ceramide, and JC-1 mitochondrial membrane potential detection kit were purchased from Biotium (Fremont, CA, USA). LYSO-ID® Green detection kit and Hoechst 33258 were purchased from Enzo Life Science (Farmingdale, NY, USA). MitoCheck® Complex II Activity Assay Kit was purchased from Cayman Chemical (Ann Arbor, MI, USA). CellTiter-Blue® Cell Viability Assay kit was purchased from Promega (Madison, WI, USA).

Cell lines. The human ovarian cancer (NCI/ADR-RES), human cervical cancer (HeLa), mouse breast carcinoma (4T1), and mouse fibroblast (NIH/3T3) cells were grown in complete growth media (DMEM

supplemented with $100 \text{ U}\cdot\text{mL}^{-1}$ penicillin, $100 \mu\text{g}\cdot\text{mL}^{-1}$ streptomycin, and 10% FBS) at 37°C in 5% CO_2 .

Synthesis and characterization of fluoroamphiphiles. The synthesis schemes were depicted in Fig. S1. For the PEGm-Fn polymers (PEG2k-F7 as an example), the F7-COOH (2.5 mmol) was activated by the EDC/NHS and reacted with L-cysteine ethyl ester hydrochloride (3 mmol) in the DCM in the presence of TEA at the room temperature overnight. The mixture was purified by the column chromatography (ethyl acetate/hexane, 1:1, v/v), affording the F7-Cys (~48% yield) as a white powder. Then, the F7-Cys was reacted with the PEG2k-MAL at a molar ratio of 1.2:1 in the DMF in the presence of TEA at the room temperature overnight. The crude product was purified by the dialysis (MWCO 1000 Da) against water for 24 h, followed by freeze drying, affording the PEG2k-F7 (~75% yield) as a white powder. For the PE-PEG2k-Fn polymers (PE-PEG2k-F7 as an example), the MAL-PEG2k-SVA (3 mmol) was reacted with the DOPE (3.3 mmol) in the DMF in the presence of TEA at the room temperature overnight. The PE-PEG2k-MAL was purified by the dialysis (MWCO 2000 Da) against water for 24 h, followed by freeze drying. Then, the F7-Cys (3.3 mmol) was reacted with the PE-PEG2k-MAL (3 mmol) in the DMF in the presence of TEA at the room temperature overnight. The final product was purified by the dialysis (MWCO 2000 Da) against water for 24 h, followed by freeze drying, affording the PE-PEG2k-F7 (~85% yield) as a white powder.

The thin layer chromatography (TLC) was developed in the mixture of the methanol and chloroform (1:4, v/v) and stained by the Dragendorff's reagent to visualize the PEG chain.¹ The ^1H NMR spectra were obtained in the deuterated solvents: DMSO-d₆, CD₃OD, or D₂O (Bruker 300 MHz). For the matrix-assisted laser desorption/ionization time of flight mass spectrometry (MALDI-TOF MS), the trans-2-[3-(4-tert-Butylphenyl)-2-methyl-2-propenylidene] malononitrile (DCTB) was used as a matrix. The polymer/DCTB mixture was deposited on a stainless-steel sample holder and analyzed on a Bruker Daltonics Microflex mass spectrometer (Billerica, MA) in the positive deflection mode.

Critical micelle concentration. The critical micelle concentration (CMC) value was determined using the pyrene as a hydrophobic fluorescent probe.² Briefly, the pyrene chloroform solution was added to the testing tubes at 8×10^{-5} M and the polymers in chloroform were added to the tubes at a 10-fold serial dilution (from 10^0 to $10^{-8} \text{ mg}\cdot\text{mL}^{-1}$). The tubes were dried under vacuum overnight, and then were hydrated by PBS and incubated with shaking at the room temperature for 24 h. The fluorescence intensity of the micelles was measured on a Tecan Infinite M1000 Pro microplate reader at the λ_{ex} 338 nm and 334 nm and λ_{em} 390 nm. The intensity ratio (I_{338 nm}/I_{334 nm}) was plotted against the polymer concentration. The CMC value was obtained as the crossover point of the two tangents of the curves.

Nanoparticle preparation and drug loading. The cargo-loaded micelles were prepared by a thin-film hydration method. Briefly, the cargos (Rh-PE or VES) and polymers were co-dissolved in the chloroform and methanol mixture, and then dried to obtain a thin cargo-polymer film under the nitrogen flow, followed by hydration with PBS. The unentrapped VES was removed by a 0.45 μ m syringe filter. The entrapped VES was quantitated by HPLC.^{3,4}

Particle size and zeta potential. The polymers were hydrated at various pHs (5.0, 7.4, or 8.5) or methanol at a final concentration of 0.1 mg·mL⁻¹. The particle size of the micelles was measured by the dynamic light scattering (DLS) on a NanoBrook 90Plus PALS Zeta Potential Analyzer (Brookhaven Instruments) at 25 °C. The zeta potential of the micelles (only in the aqueous buffers) was measured by the same instrument.

Nanoparticle morphology. The morphology of the micelles was examined using the transmission electron microscopy (TEM). Briefly, one drop of the micellar dispersion was placed on a 400-mesh carbon-coated copper grid (Ted Pella, Inc.). The micrograph was recorded on a JEOL JEM-2010 TEM (JEOL, Japan).

Fluorescence resonance energy transfer (FRET). The micelle stability and the lipid fusion were studied by the FRET.⁵ For the micelle stability study, the polymeric micelles containing 2% of the dye pair, DiI/DiO (1:1, w/w), were incubated in the PBS or mouse serum at 37 °C for 16 days. The time-resolved spectra were recorded at the λ_{ex} 484 nm and λ_{em} from 490 nm to 700 nm on a microplate reader. To study the lipid membrane fusion, the polymers were incubated with the DPPC liposomes (half of the liposomes containing 2% DiI/DiO) at the pH of 5.0 or 7.4 at 37 °C for 72 h. The time-resolved spectra were recorded at the λ_{ex} 484 nm and λ_{em} from 490 nm to 700 nm.

Cellular uptake. The lissamine rhodamine B-phosphatidylethanolamine (Rh-PE) (1%, w/w) was used as a fluorescent probe to label the fluoroamphiphile micelles. For better comparison, the TAT-modified micelles (TAT-PEG2k-PE/PEG2k-PE) and the PEG2k-F7 containing micelles (PEG2k-F7/PEG2k-PE) at the polymer ratios of 0:100, 10:90, 50:50, or 100:0 (mol/mol) were prepared, respectively.

Before the experiment, the cells were seeded at a density of 1×10^5 cells/well in 24-well plates for 24 h. The cells were incubated with the micelles in a serum-free medium for 1 h. Then, the cells were washed three times by PBS to remove the uninternalized micelles/dyes. For the microscopy, the cells were observed on a Nikon Ti Eclipse fluorescence microscope system. For the flow cytometry, the cells were trypsinized and resuspended in 400 μ L PBS, followed by the analysis on a BD Accuri C6 flow cytometer. The dead cells and cell debris were excluded from the viable cells using the forward *versus* side scatter. To study the uptake pathways, the cellular uptake at 37 °C was compared with that at 4 °C. In addition, the cells were

pre-incubated with the endocytosis inhibitors, chlorpromazine hydrochloride, nystatin, or HP- β -CD at 37 °C for 0.5 h, and then incubated with the micelles at 37 °C for 1 h. The uptake efficiencies under these conditions were compared.

Subcellular localization and mitochondrial targeting. The cells were seeded at a density of 1×10^5 cells/well for 24 h. The cells were incubated with the Rh-PE-labeled micelles in the serum-free medium at 37 °C. The intracellular compartments were stained by the following commercial dyes using the vendors' recommended protocols. Then, the cells were analyzed on a Nikon Ti Eclipse confocal microscope system.

To study the endocytosis, the living cells were stained by the LYSO-ID® Green to visualize the endosomes/lysosomes. To study the intracellular localization pattern, the mitochondrion was stained by the Rh123 or MitoView™ Green; the endoplasmic reticulum was stained by the ER-Tracker™ Green; and the Golgi apparatus was stained by the NBD C6-ceramide. To study the mechanisms of the mitochondrial targeting, the polymers or their components were labeled by the fluorescein isothiocyanate (FITC). They were pre-normalized to the same fluorescence intensity and then incubated with the HeLa cells at 37 °C for 1 h. The mitochondria were stained by the MitoView™ 633. To visualize the cell nuclei, the cells were incubated with the Hoechst 33258 for 15 min.

Mitochondrial membrane potential. The mitochondrial membrane potential was determined by the JC-1 dye and analyzed by flow cytometry. Briefly, the cells were seeded at a density of 1×10^5 cells/well in 24-well plates for 24 h. The cells were incubated with the PEG2k-F7, TPP, and CCCP at 50 μ M in the serum-free medium for 1 h, respectively. Then, the cells were washed by the iced-cold medium to remove the uninternalized materials. The cells were incubated with the JC-1 dye at 37 °C for 15 min, followed by flow cytometry.

Mitochondrial isolation. The mitochondria were isolated by the Mitochondria Isolation Kit for Cultured Cells (Thermo Fisher Scientific). Briefly, 2×10^7 HeLa cells were collected by the trypsinization and centrifugation. Then, the cells were lysed and the mitochondria were separated from other cell fragments by several washing and centrifugation steps as the manufacturer's manual (Option A). The isolated mitochondria were characterized by their morphology, particle size, zeta potential, and reactive oxygen species (ROS) production capability.⁶

Quantification of the mitochondria-accumulated dyes. 2×10^7 HeLa cells were incubated with the fluorescent polymers at 37 °C for 1 h. After washing with PBS, the (total) cellular fluorescence intensity was measured by a microplate reader. Then, the cells were lysed and the mitochondria were separated from

other cell fragments by the Mitochondria Isolation Kit (Option A). The fluorescence intensities of the isolated mitochondria and other cell fragments were measured by a microplate reader. To study the influence of the mitochondrial depolarization on the mitochondrial targeting, the cells were pre-incubated with the uncoupler, CCCP (50 µM), for 1 h, and then incubated with the fluorescent polymers.

Binding affinity with the isolated mitochondria. The isolated mitochondria were incubated with the FITC-labeled polymers or commercial dyes at 37 °C for 1 h. The mitochondria were washed by PBS for three times, collected by the centrifugation, and resuspended in 200 µL PBS. The mitochondrial suspension was observed on a Nikon Ti Eclipse fluorescence microscope. The fluorescence intensity was measured by a microplate reader. For the competitive binding assay, the isolated mitochondria were pre-incubated with either the TPP or PEG2k-F7 at 37 °C for 1 h. Then, the pretreated mitochondria were washed by PBS for three times, followed by incubation with the Rh123 at 37 °C for 1 h. After washing with PBS, the fluorescence intensity of the mitochondria-associated Rh123 was quantitated.

Polymer-lipid binding. The interaction/affinity of the polymers and various phospholipids was investigated by flow cytometry, a protocol used for studying the protein-lipid interaction.⁷ The liposomes containing 90% of the phospholipids (DOPE, DPPC, DPPG, DPPS, DOTAP or cardiolipin) and 10% of the cholesterol and the “mitochondrial membrane-mimicking” liposomes⁸ containing the phospholipids (DPPC:DOPE, 5/3, w/w) (90%-50%), cardiolipin (0%-40%), and cholesterol (10%), were prepared by the thin-film hydration method followed by extrusion¹. The liposomes’ particle size and zeta potential were determined. The liposomes were incubated with the FITC-labeled polymers/lipids (or Rh123) at 37 °C for 1 h, followed by flow cytometry.

In vitro drug release. The VES release rate from the polymeric micelles was determined by a dialysis method.⁹⁻¹¹ Briefly, the VES-loaded polymeric micelles were dialyzed (MWCO 12000-14000 Da) against PBS (containing 0.5% Tween 80 to maintain the “sink” condition) at 37 °C. The released drug was determined by HPLC.^{3, 4}

Cellular ROS production. The ROS production was determined using the 2',7'-dichlorodihydrofluorescein diacetate (H₂DCFDA).¹² Briefly, the HeLa cells were seeded in 12-well plates at 1.0×10^5 cells/well and incubated at 37 °C overnight before the experiment. The cells were incubated with various formulations for 20 h. After washing with PBS, the treated cells were incubated with the H₂DCFDA (10 µM) at 37 °C for 0.5 h, followed by fluorescence microscopy.

Cytotoxicity in the monolayer cells. The cells were seeded in 96-well plates at 2×10^3 cells/well 24 h

before the treatment. The polymers, VES, or VES-loaded micelles were incubated with the cells in the complete growth medium at 37 °C for 48 h. The cell viability was determined by the CellTiter-Blue® Cell Viability Assay (Promega). Briefly, 10 µL of the CellTiter-Blue® reagent was diluted with 90 µL of the complete growth medium per well and incubated with the cells at 37 °C for 2 h. Thereafter, the fluorescence intensity was measured at the λ_{ex} 560 nm and λ_{em} 590 nm on a microplate reader.

Activity of the mitochondrial complex II (CII). The CII activity was determined by the MitoCheck® Complex II Activity Assay Kit (Cayman Chemical). Briefly, the CII inhibitor, 2-thenoyltrifluoroacetone (TTFA, 1 mM), was used as a positive control. To prevent the interference from other electron transport chain (ETC) complexes, the rotenone (1 µM, CI inhibitor), antimycin A (10 µM, CIII inhibitor), and potassium cyanide (2 mM, CIV inhibitor) were present as the nonspecific inhibitors. Briefly, the HeLa cells were seeded in 12-well plates at 1.0×10^5 cells/well and incubated at 37 °C overnight before the experiment. The cells were incubated with various formulations or inhibitors for 1 hour, then the mitochondria were isolated for the CII activity assay as the manual.

Establishment of the cancer cell spheroids. The HeLa cell spheroids were established by a well-developed method.^{10, 13} Briefly, the 96-well plate was pre-coated with the agarose in the culture medium (1.5%, w/v), followed by gelation at the room temperature. The cells were seeded in the pre-coated plate at 5×10^3 cells/well. The plate was then centrifuged for 15 min at 1,500 rcf and incubated at 37 °C in 5% CO₂ for the spheroid formation.

Penetration through the cell spheroids. The 4-5 day cell spheroids were incubated with the Rh-PE-labeled micelles for 4 h. After treatments, the spheroids were transferred to a new plate and gently washed with PBS. Then, the spheroids were observed on the confocal microscope. Z-stack images were obtained at an interval of 20 µm.

Cytotoxicity and growth inhibition in the cell spheroids. The cell spheroids were incubated with various formulations for 72 h. The cell viability was determined by the CellTiter-Blue®Cell Viability Assay.¹² Briefly, 20 µL of the reagent was diluted with 180 µL of the fresh complete growth medium and incubated with the cell spheroids at 37 °C for 12 h. The fluorescence intensity was measured by a microplate reader. In addition, the spheroids' size and morphology were analyzed by the microscope to estimate the spheroid growth inhibition.

Establishment of the *in vivo* tumor model. The 4-week old female BALB/c mice were purchased from the Envigo RMS, LLC. All animal procedures were performed according to an animal care protocol

approved by the Texas A&M University Institutional Animal Care and Use Committees (IACUC). The mice were housed in groups of five per cage at 19 - 23 °C with a 12 h light - dark cycle and allowed free access to food and water. The syngeneic 4T1 tumor model was established by the subcutaneous (s.c.) implantation of 5×10^6 4T1 cells in the mouse abdominal mammary fat pad.¹⁴ The tumor was monitored every other day for the length (l) and width (w) of the tumor by a caliper and the tumor volume was calculated by the equation $V = (l \times w^2)/2$.

In vivo biodistribution, cellular uptake, and mitochondrial accumulation. When the tumor was around 400 mm³, the free Rh-PE (25 µg) or Rh-PE-labeled micelles were intravenously (i.v.) injected in the mice *via* the tail vein. At 2, 8 and 24 h after the injection, the mice were sacrificed and the tumor, blood, and major organs (heart, liver, spleen, lung, and kidney) were collected.

To determine the biodistribution, the tissues were lysed by probe sonication in the presence of 2% Triton X-100. The dye was extracted by methanol and the fluorescence intensity was measured at the λ_{ex} 560 nm and λ_{em} 590 nm on a microplate reader.

To determine the cellular uptake in the tumor, the tumor tissues were minced into small pieces and incubated in the Collagenase D (1 mg·mL⁻¹) solution at 37 °C for 30 min to dissociate the tumoral cells. The single-cell suspension was analyzed immediately by flow cytometry.^{11, 15}

To determine the mitochondrial accumulation in the tumor cells, the mitochondria were isolated from the aforementioned dissociated cells by the Mitochondria Isolation Kit. The isolated mitochondria were washed by PBS and re-suspended in 400 µL PBS, followed by flow cytometry.

In vivo anticancer activity. As the tumor reached around 100 mm³, the saline, free VES, free PEG2k-F7, VES-loaded PEG2k-PE micelles, or VES-loaded PEG2k-F7 micelles were injected intravenously *via* the tail vein at a dose of 20 mg·kg⁻¹ VES every 4 days (3 injections in total). The dose of the free PEG2k-F7 was equivalent to that of the VES-loaded micelles. The tumor size and mouse body weight were monitored every other day. On day 14 after the first injection, the mice were sacrificed and the blood, tumor, and major organs were collected. The white blood cells were counted by a hemocytometer. The activities of creatinine, alanine transaminase (ALT), and aspartate transaminase (AST) were measured by the assay kits (Teco Diagnostics). The tissues were sectioned and stained by the hematoxylin and eosin (H&E).

Statistical analysis. Data were expressed as mean ± standard deviation (SD) and analyzed by the t-test using the GraphPad Prism 6.0. P < 0.05 is statistically significant.

Supporting Figures

Fig. S1. Synthesis schemes of the fluoroamphiphiles. (A) Synthesis of the Fn-Cys. (B) Synthesis of the PE-PEG2k-Fn. (C) Synthesis of the PEGm-Fn. (Fn: F3, F5, F7, or F9; PEGm: PEG1k, PEG2k, or PEG5k)

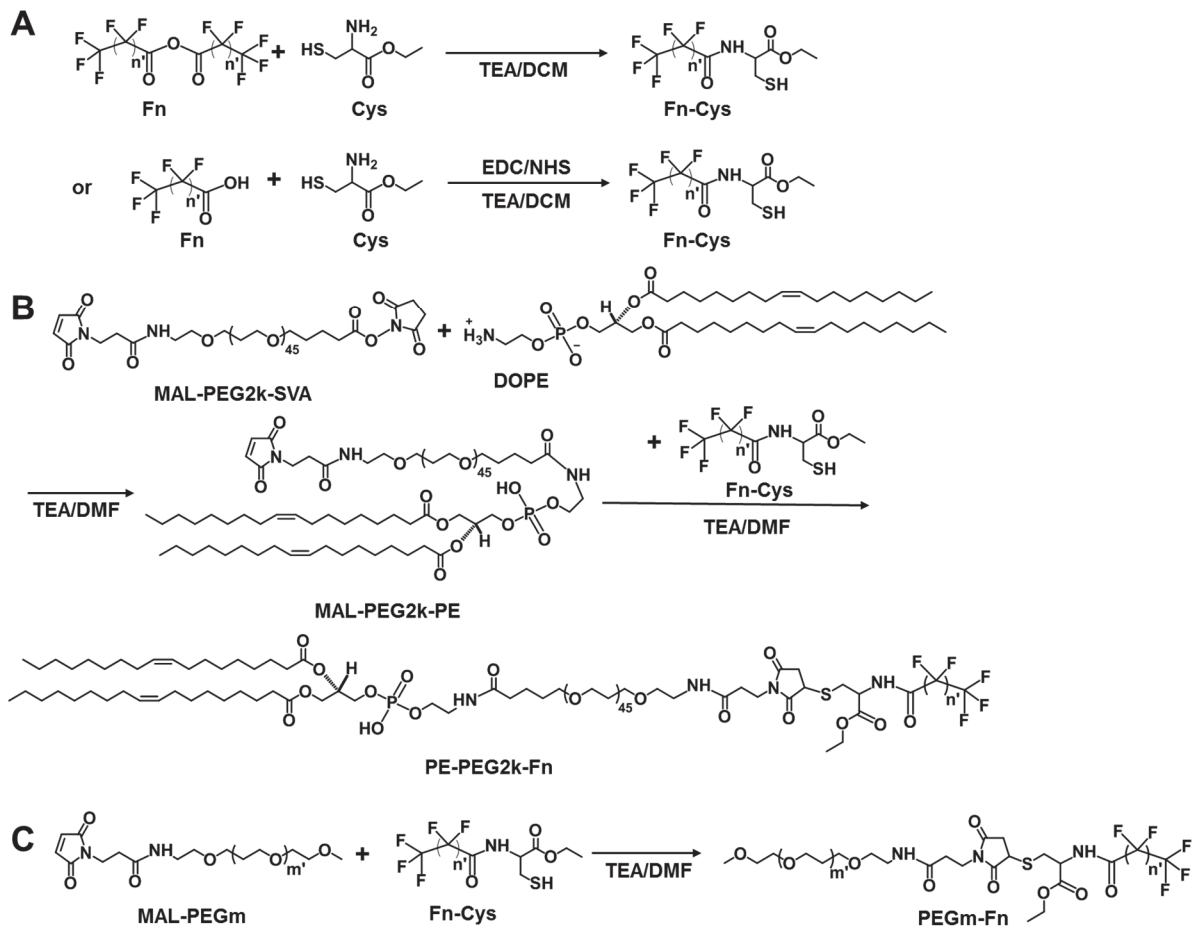


Fig. S2. Effect of the fluoroamphiphiles on the lipid membrane fusion at pH 7.4, determined by the fluorescence resonance energy transfer (FRET). (A) Schematic illustration of the lipid bilayer fusion experiment. (B) Illustration of the data processing. The FRET spectra were converted to the plots of the intensity of the emission peaks (501 and 565 nm) over time, for easy comparison. The equilibrium was reached when the curves leveled off. (C) The FRET results at pH 7.4. Polymer concentration: 0.1 mg·mL⁻¹. DPPC liposome concentration: 2 mg·mL⁻¹. FRET dye pair: DiO (20 µg·mL⁻¹) as the donor and DiI (20 µg·mL⁻¹) as the acceptor. DPPC, 1,2-dipalmitoyl-sn-glycerol-3-phosphocholine. MFI, mean fluorescence intensity.

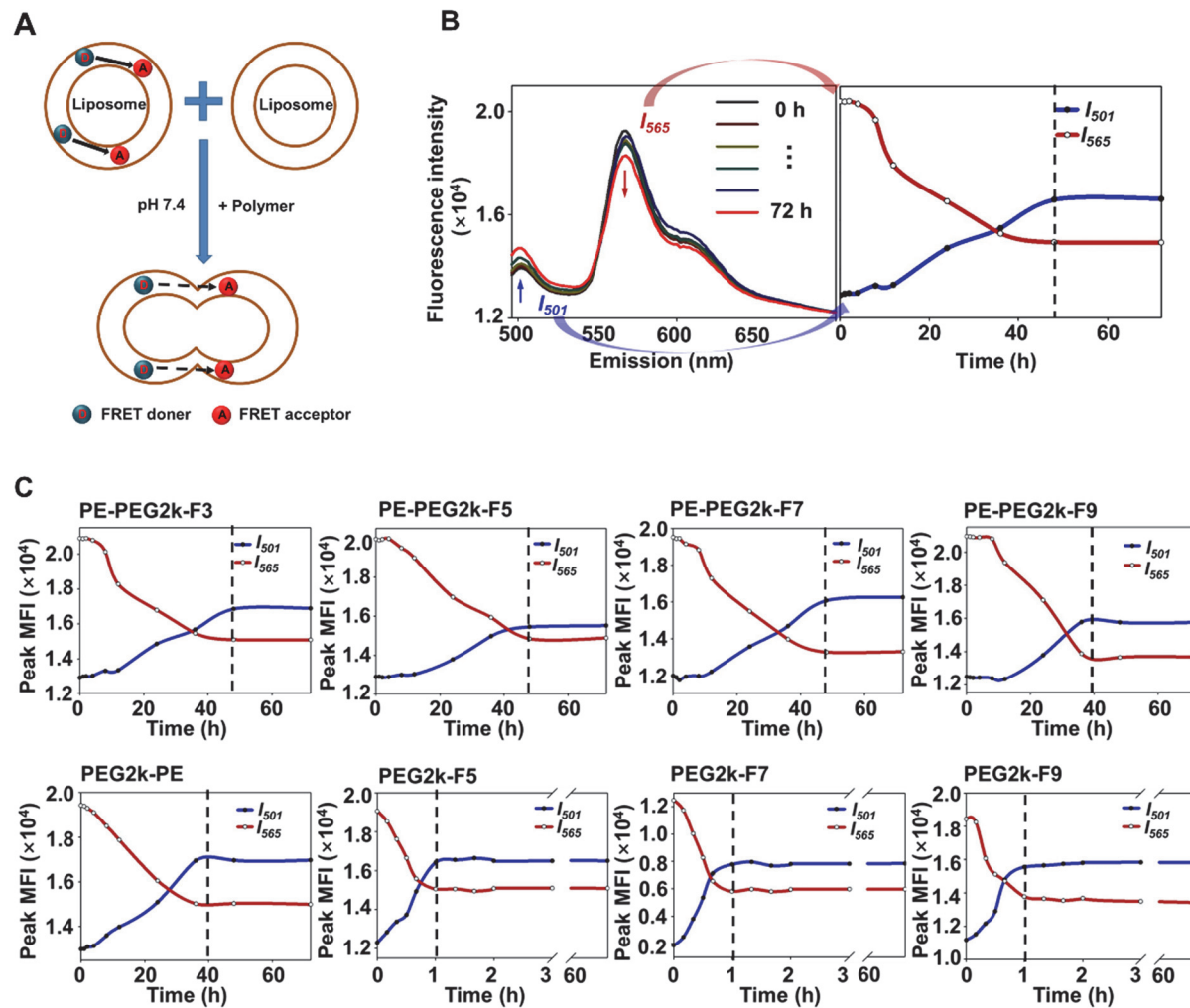
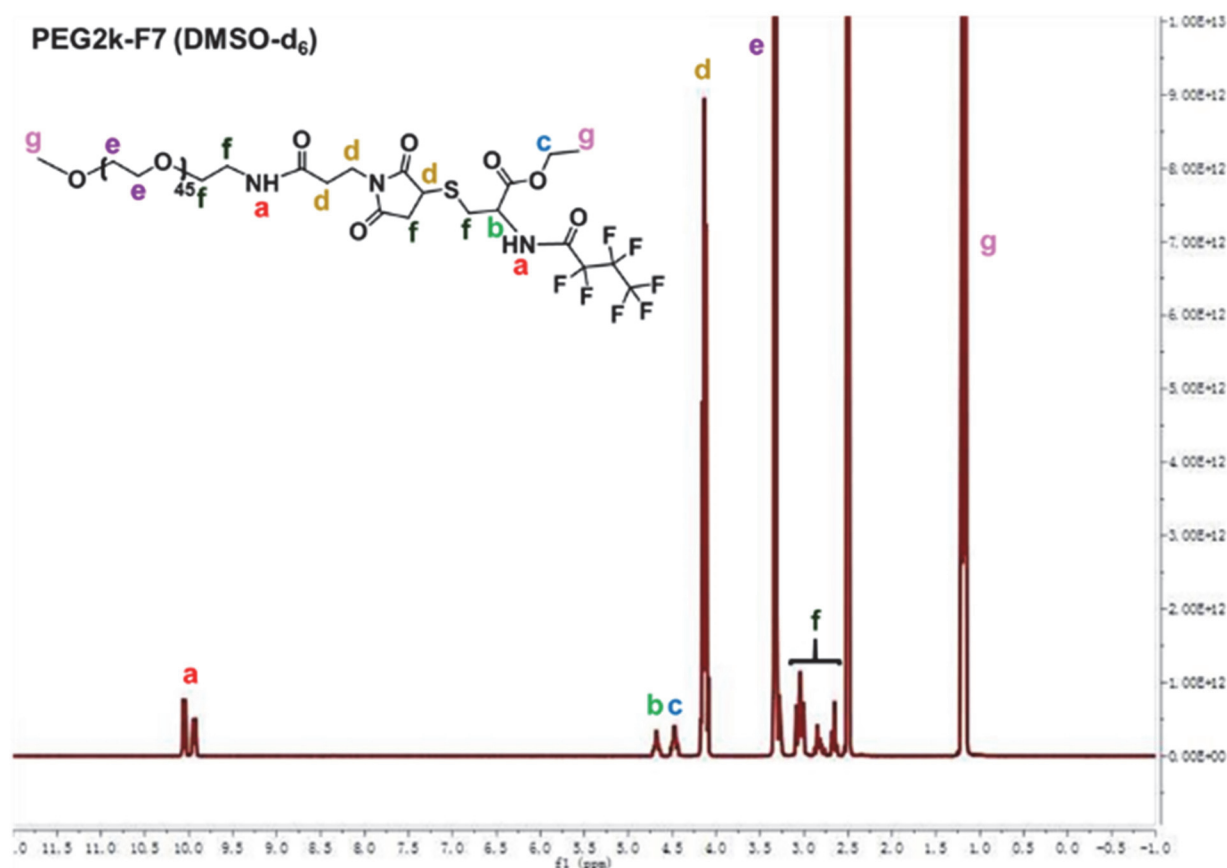


Fig S3. Thin layer chromatography (TLC) of the PEG2k-F7. The TLC plate was developed in the chloroform/methanol mixture (4:1, v/v) and stained to visualize the PEG by the Dragendorff's reagent. The PEG's shift was slowed down by the F7, indicating the successful reaction.

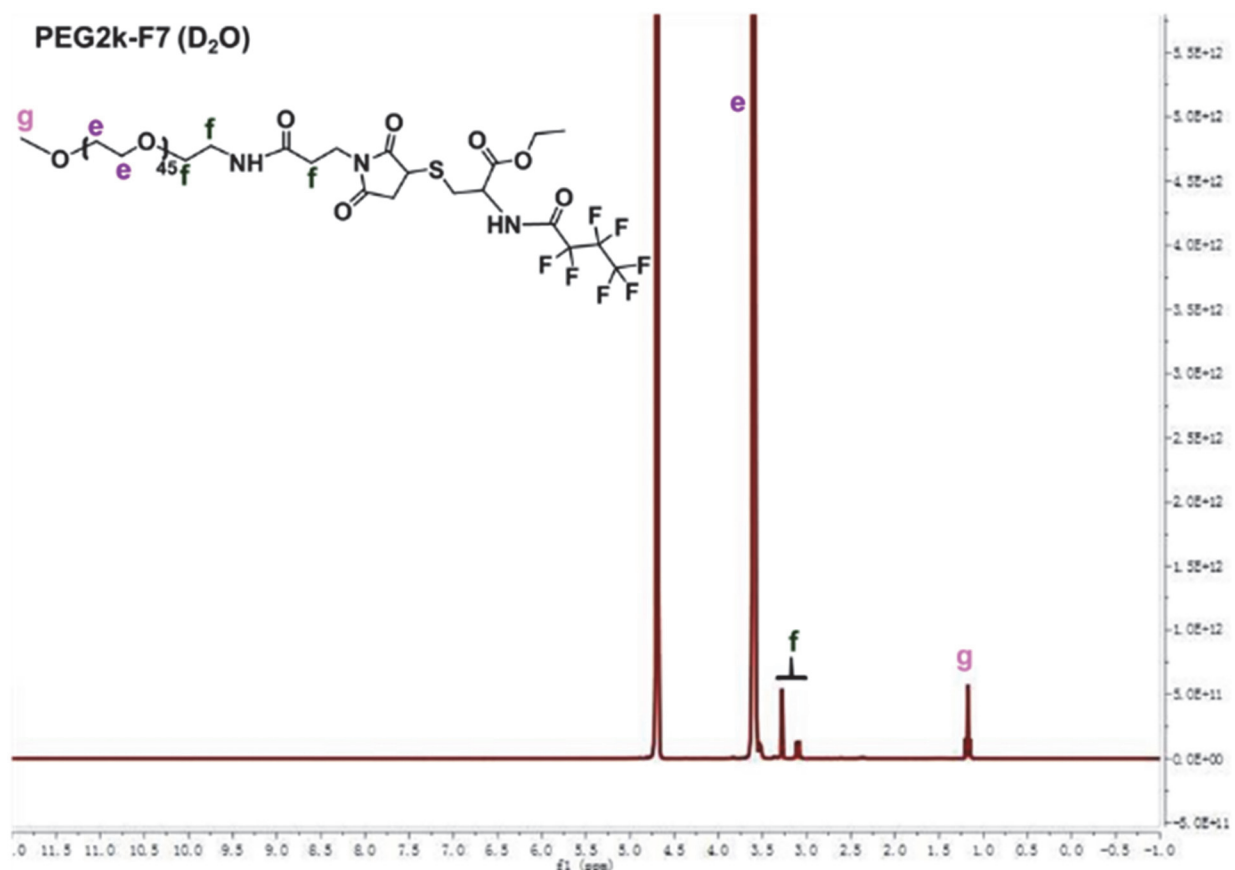


Fig. S4. ^1H -Nuclear Magnetic Resonance ($^1\text{H-NMR}$) spectra of the PEG2k-F7 in the DMSO-d₆ (A), D₂O (B), or CD₃OD (C).

A



B



C

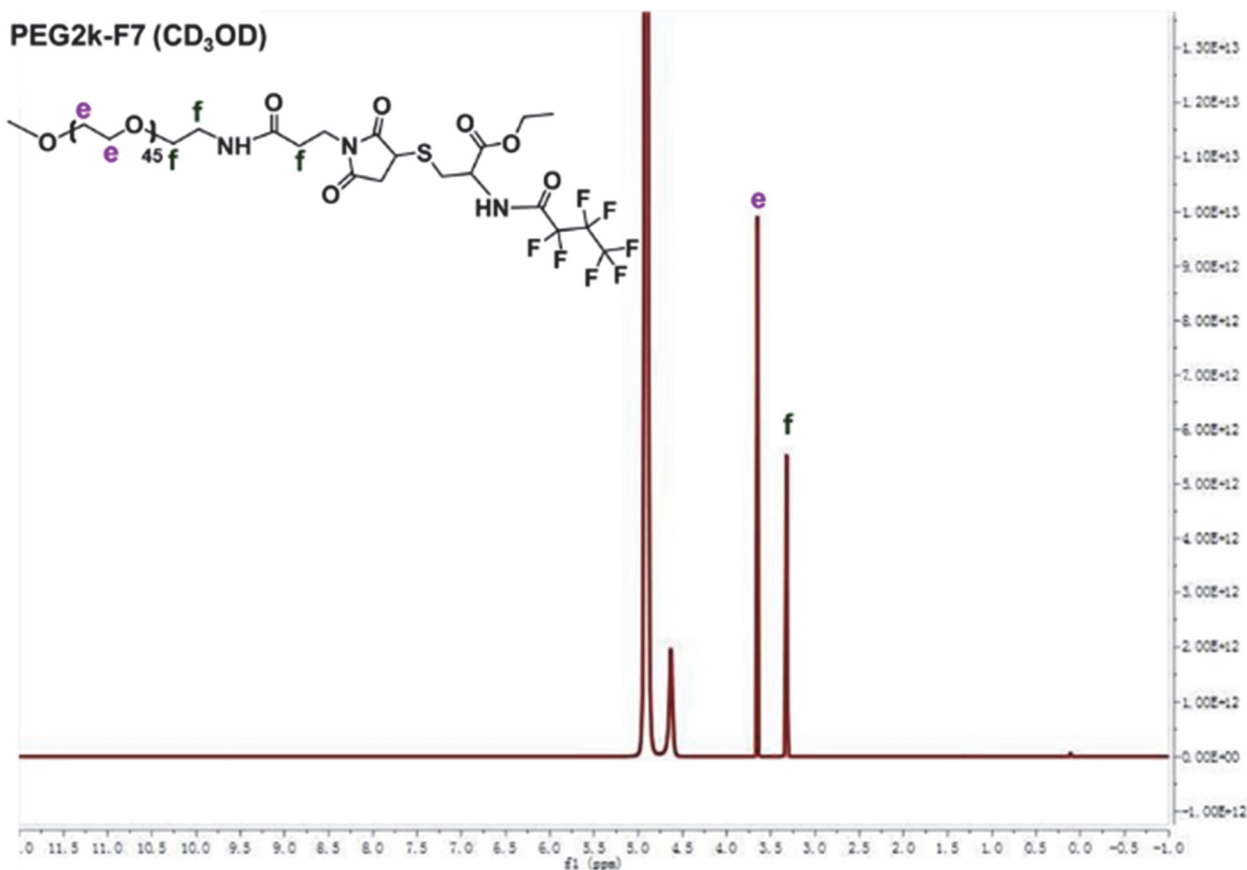


Fig. S5 Molecular weight of the PEG2k-F7, determined by the matrix-assisted laser desorption/ionization time of flight mass spectrometry (MALDI-TOF MS) using the DCTB as a matrix in the positive deflection mode.

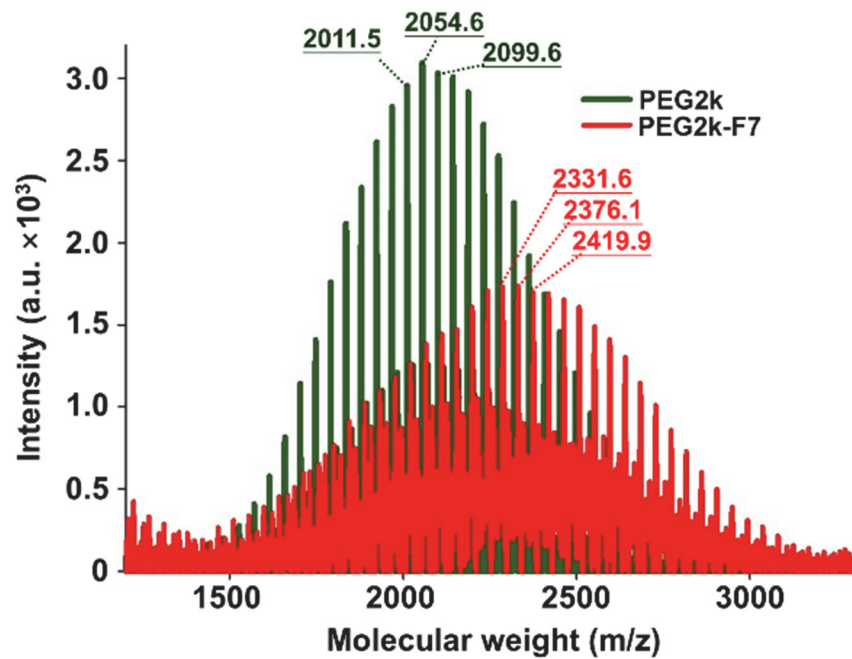


Fig. S6 Critical micelle concentration (CMC) values of the PEGm-F7 ($m=1k$, $2k$, or $5k$), determined in PBS using the pyrene as a fluorescent probe.

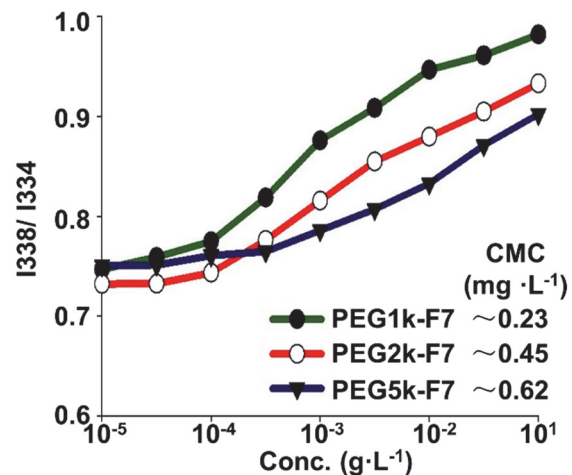


Fig. S7 Morphology of the PEG2k-F7 assembled micelles, detected by the transmission electron microscopy (TEM).

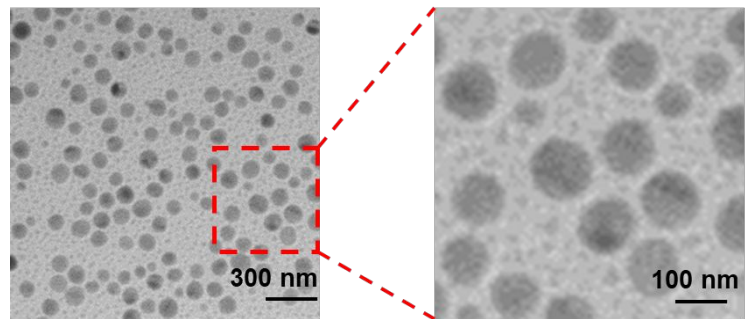


Fig. S8 Particle sizes of the PEGm-F7 assembled micelles ($m=1k$, $2k$, or $5k$) at various pHs or in the methanol, determined by the dynamic light scattering (DLS).

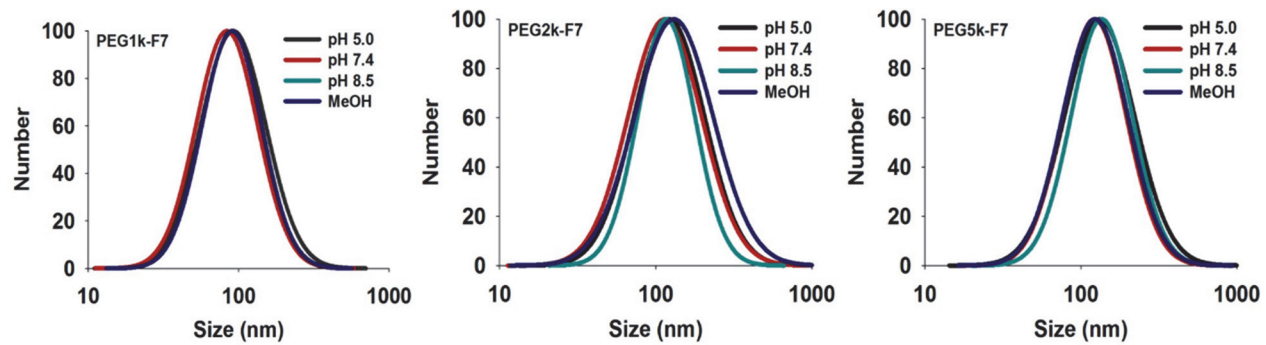


Fig. S9 Zeta potentials of the PEGm-F7 ($m=1k$, $2k$, or $5k$) and PEG2k-PE at various pHs. Data were expressed as the mean \pm SD.

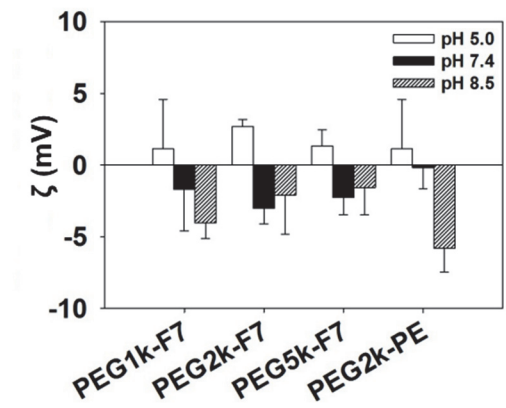


Fig. S10 Stability of the PEGm-F7 micelles ($m=1k$, $2k$, or $5k$), determined by the FRET. The FRET dye pair (DiO/DiI) was loaded to the micelles. The micelles were incubated at 37°C in the PBS or mouse serum. MFI, mean fluorescence intensity.

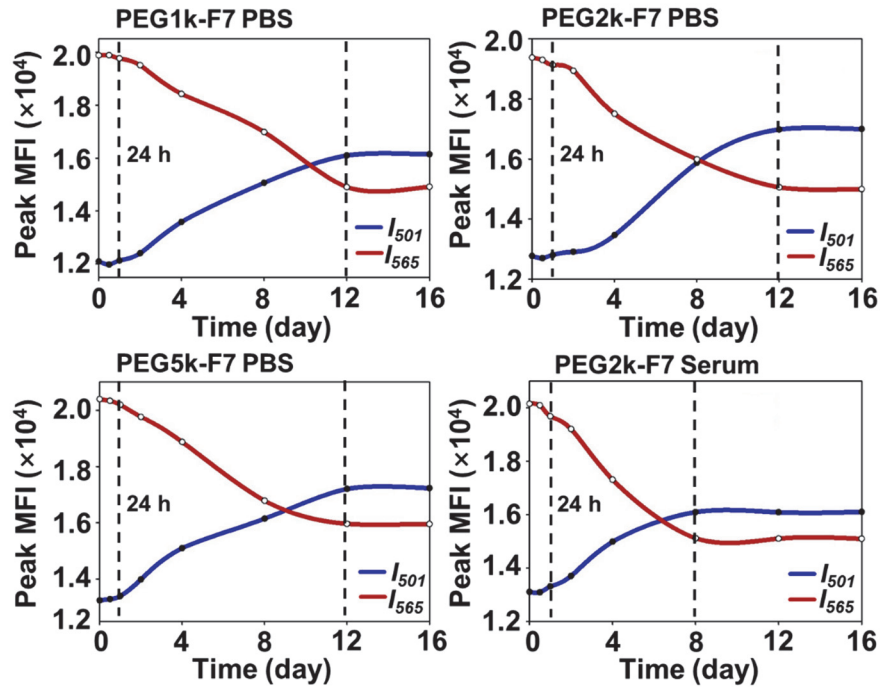


Fig. S11 Cellular uptake of the Rh-PE-loaded micelles in the HeLa, NCI/ADR-RES, and NIH/3T3 cells, determined by fluorescence microscopy (A) and flow cytometry (B). Incubation time: 1 h. MFI, mean fluorescence intensity. Data were expressed as the mean \pm SD.

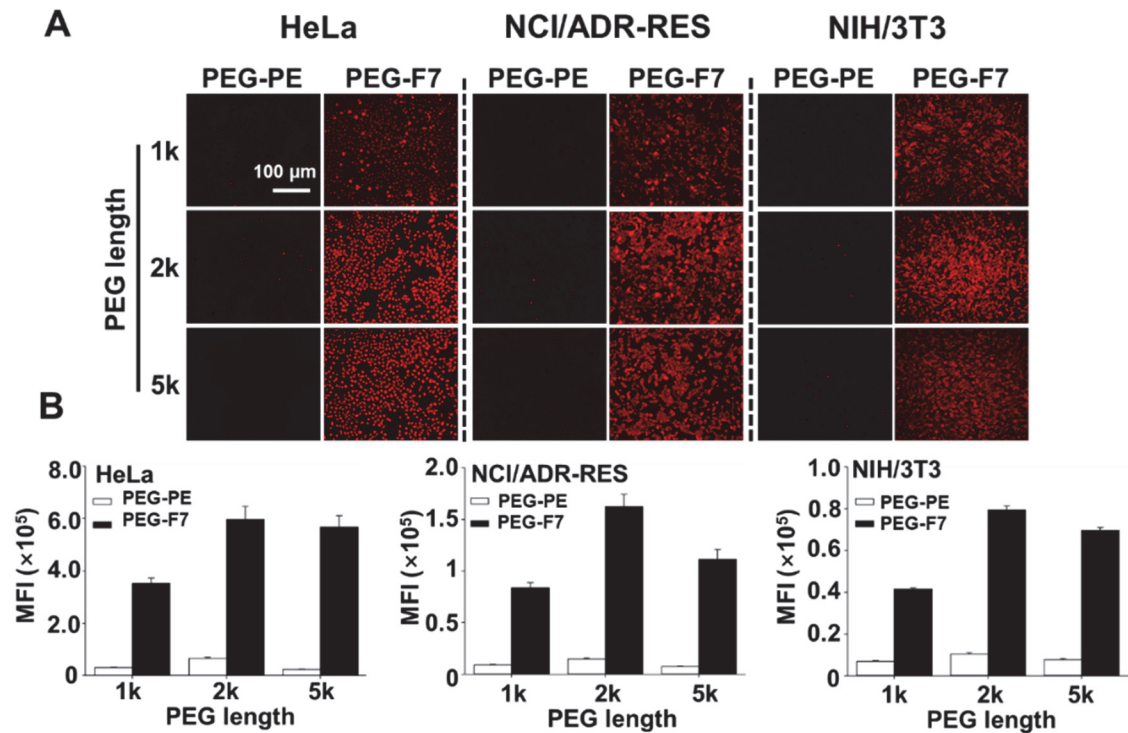


Fig. S12 Cellular uptake of the Rh-PE-loaded polymeric micelles, determined by flow cytometry (A) and fluorescence microscopy at the 100% modification (B). The PEG2k-PE micelles were modified by the PEG2k-F7 (F7) or TAT-PEG2k-PE (TAT) at the indicated ratios. Cell line: HeLa cells. Incubation time: 1 h. MFI, mean fluorescence intensity. Data were expressed as the mean \pm SD.

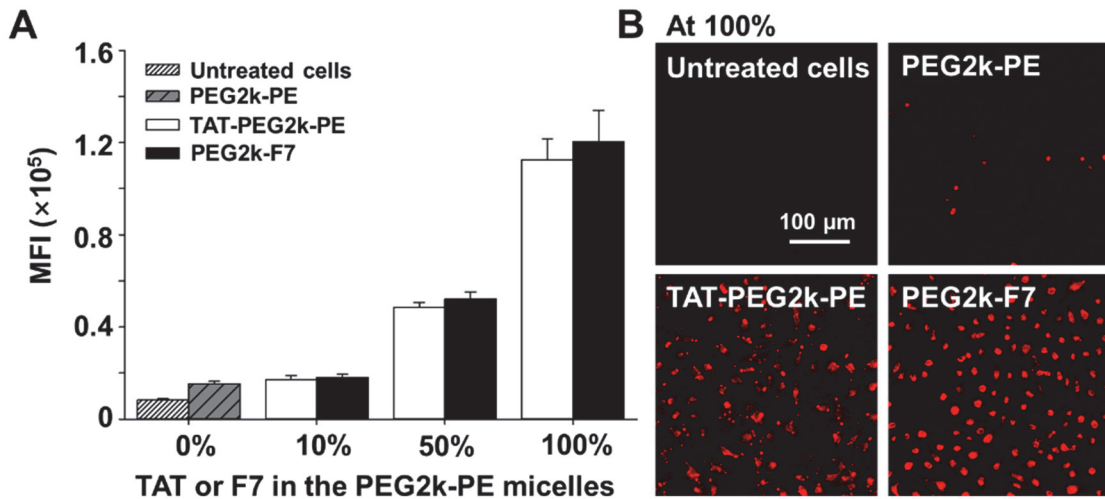


Fig. S13 Cellular uptake in the presence of the endocytosis inhibitors, determined by flow cytometry. The cells were pre-incubated with the nystatin (A) or 2-hydroxypropyl- β -cyclodextrin (HP- β -CD) (B) for 0.5 h, and then incubated with the Rh-PE-loaded micelles for 1 h. Cell line: HeLa cells. MFI, mean fluorescence intensity. Data were expressed as the mean \pm SD.

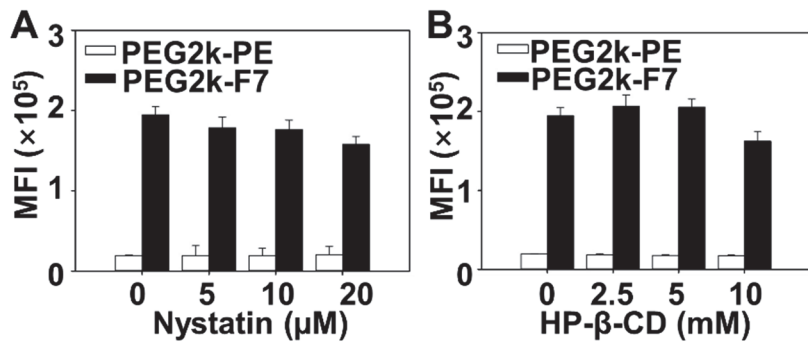


Fig. S14 Fusion of the DPPC liposomes in the presence of the PEG2k-PE at pH 7.4 (A) and pH 5.0 (B), determined by the FRET (dye pair: DiI/DiO). The protocol was depicted in Fig. S2. MFI, mean fluorescence intensity. Note: Fusion of the liposomes in the presence of the PEG2k-F7 can be found in Fig. 2D.

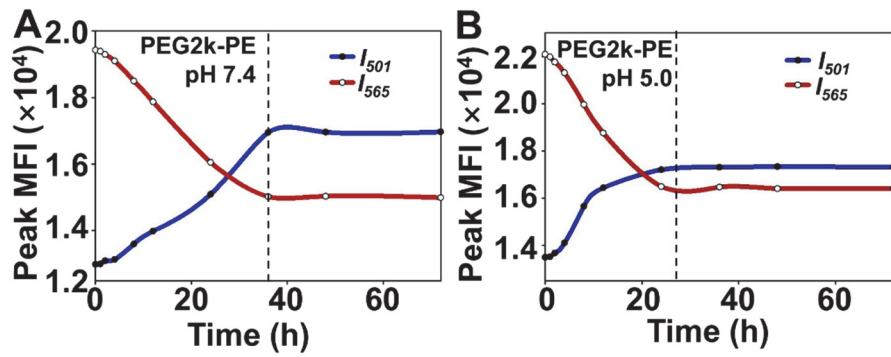


Fig. S15 Intracellular localization of the Rh-PE-loaded PEG2k-F7 micelles at 5, 30 and 60 min, determined by confocal microscopy. Mitochondria were stained by the MitoView™ Green. Cell nuclei were stained by the Hoechst 33258. Cell line: HeLa cells.

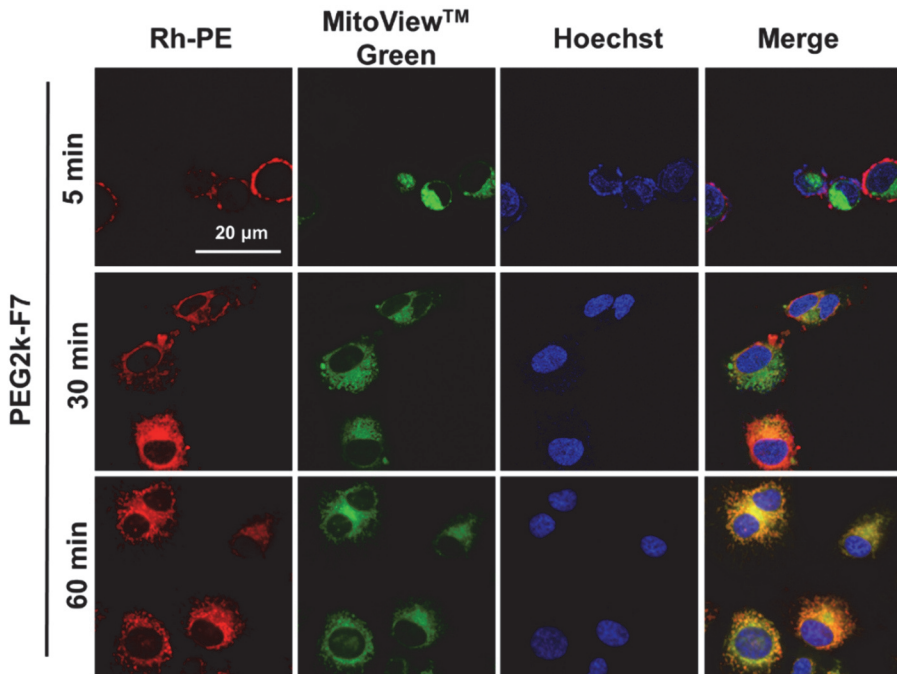
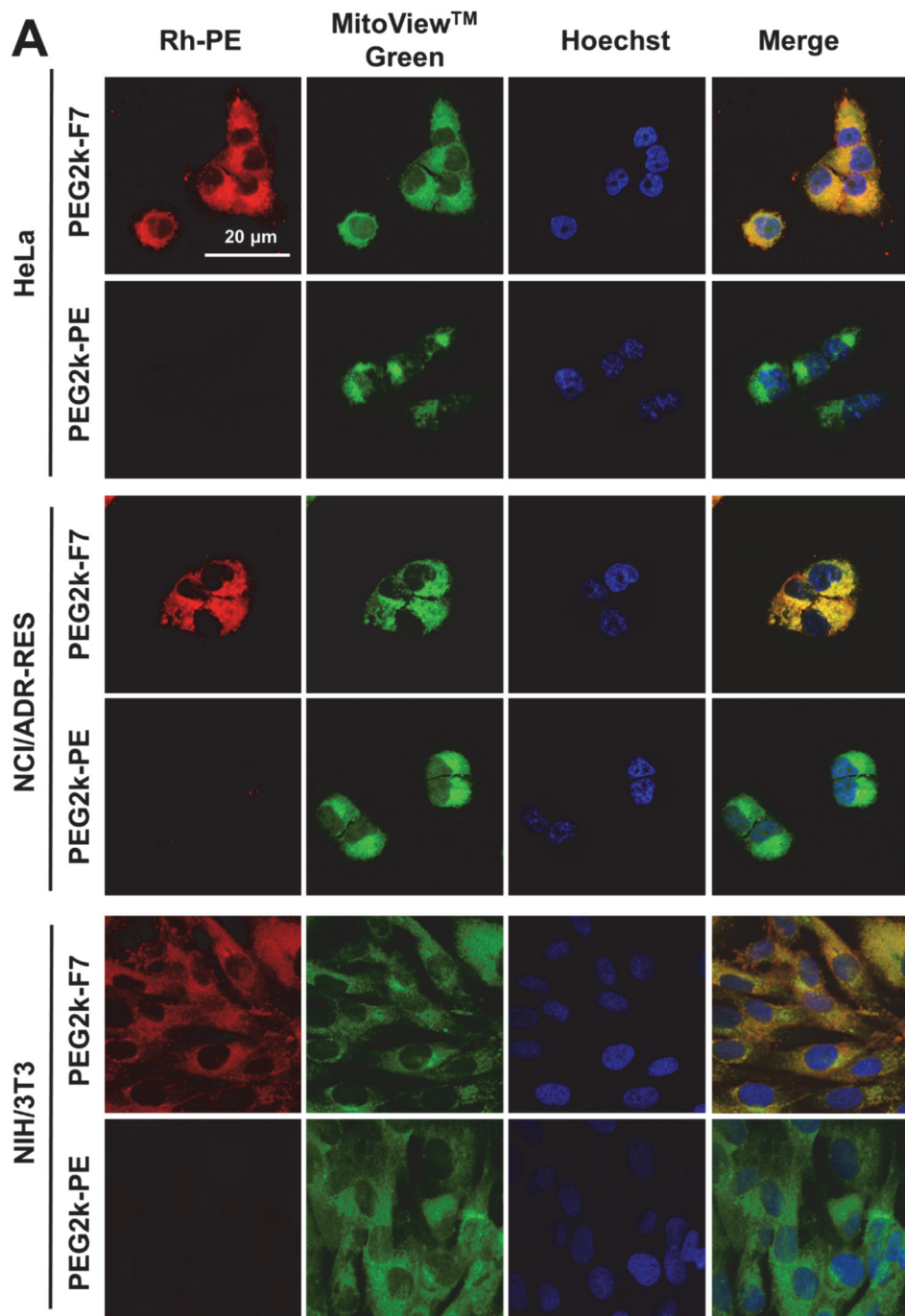


Fig. S16 Mitochondrial accumulation of the Rh-PE-loaded micelles in various cell lines, determined by confocal microscopy. Mitochondria were stained by the MitoView™ Green (potential-independent dye) (A) or Rh123 (potential-dependent dye) (B). Cell nuclei were stained by the Hoechst 33258. Incubation time: 1 h.



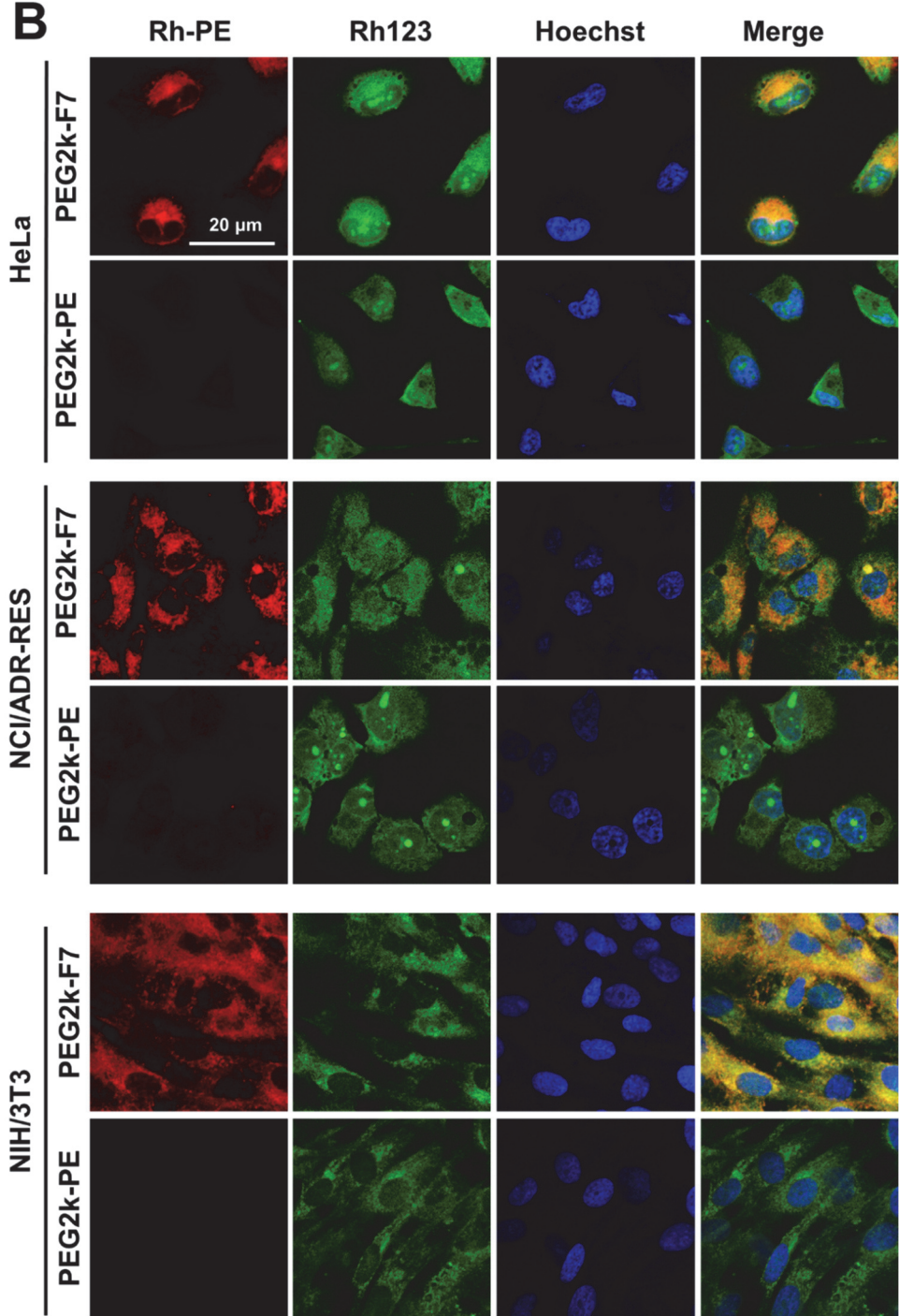
B

Fig. S17 Intracellular localization of the Rh-PE-loaded micelles, FITC-labeled PEG2k-F7, and Rh-PE in the HeLa cells, determined by confocal microscopy. Mitochondria were stained by the MitoView™ Green or MitoView™ 633. Cell nuclei were stained by Hoechst 33258. Cell line: HeLa cells. Incubation time: 1 h.

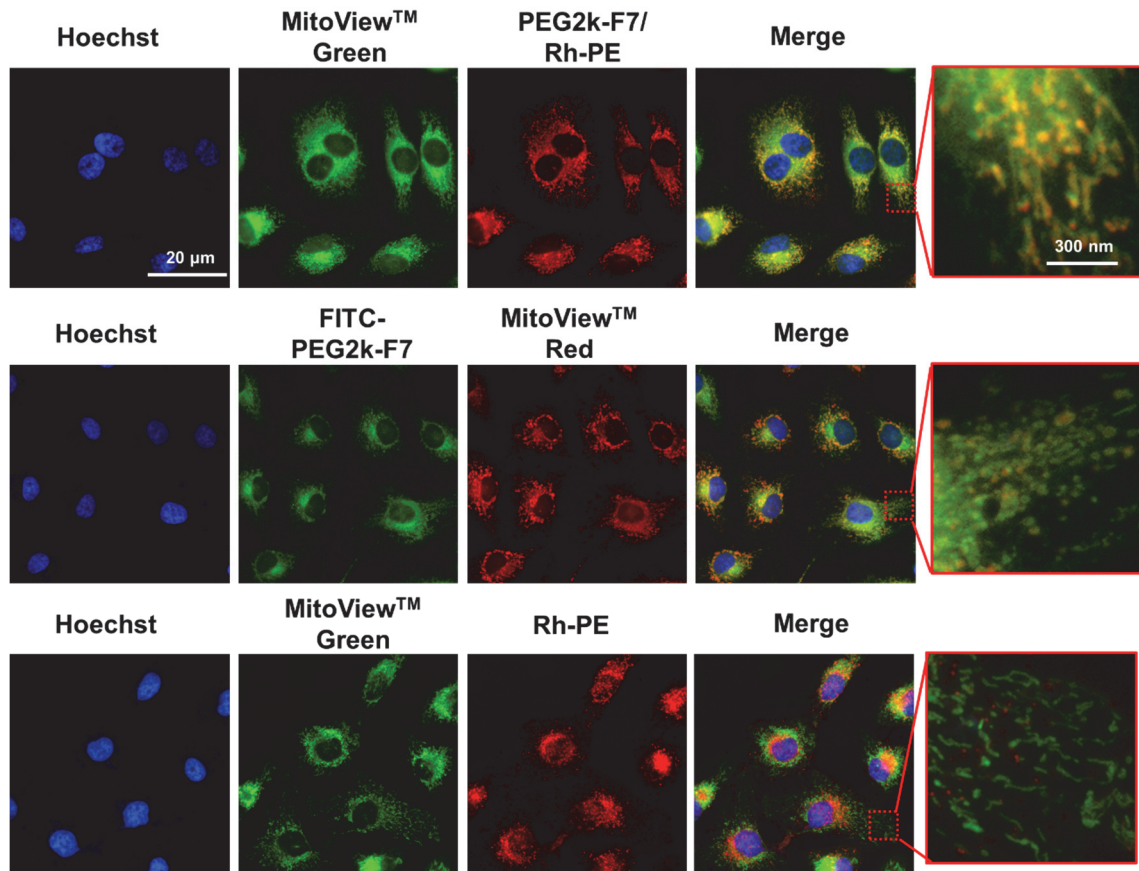


Fig. S18 Epifluorescence of the HeLa cells treated by the fluorescein isothiocyanate (FITC)-labeled materials. Mitochondria were stained by the MitoView™ 633 (red). Cell nuclei were stained by the Hoechst 33258. Cell line: HeLa cells. Incubation time: 1h.

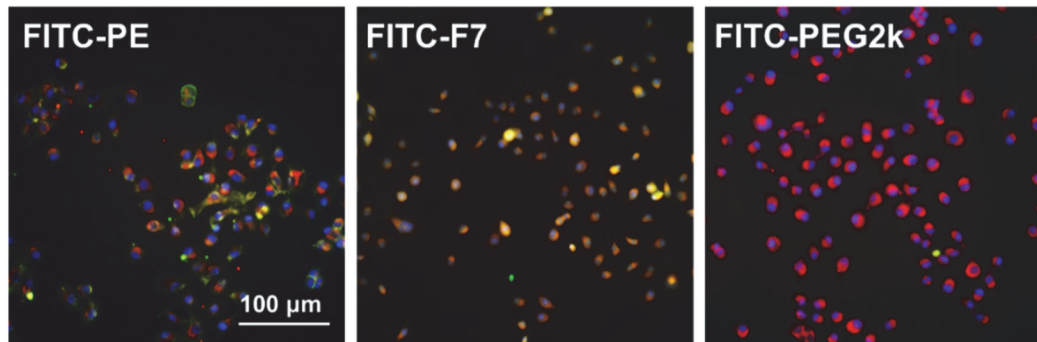


Fig. S19 Mitochondrial localization of the Rh-PE-loaded PEG2k-F7 micelles with or without the CCCP pretreatment. Mitochondria were stained by the MitoView™ Green. Cell nuclei were stained by Hoechst 33258.

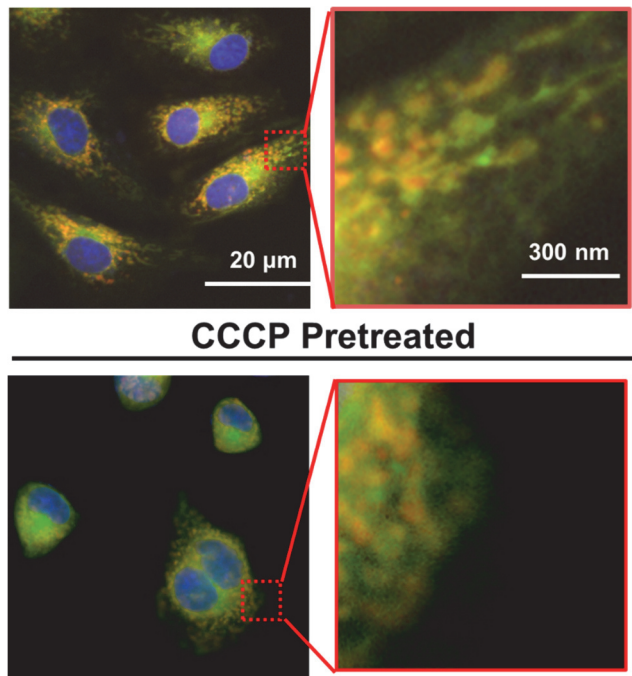


Fig. S20 Characterization of the isolated mitochondria from the Hela cells. (A) Morphology (confocal microscopy); (B) Particle size; (C) Zeta potential; and (D) ROS production (determined by the H₂DCFDA). Data were expressed as the mean \pm SD.

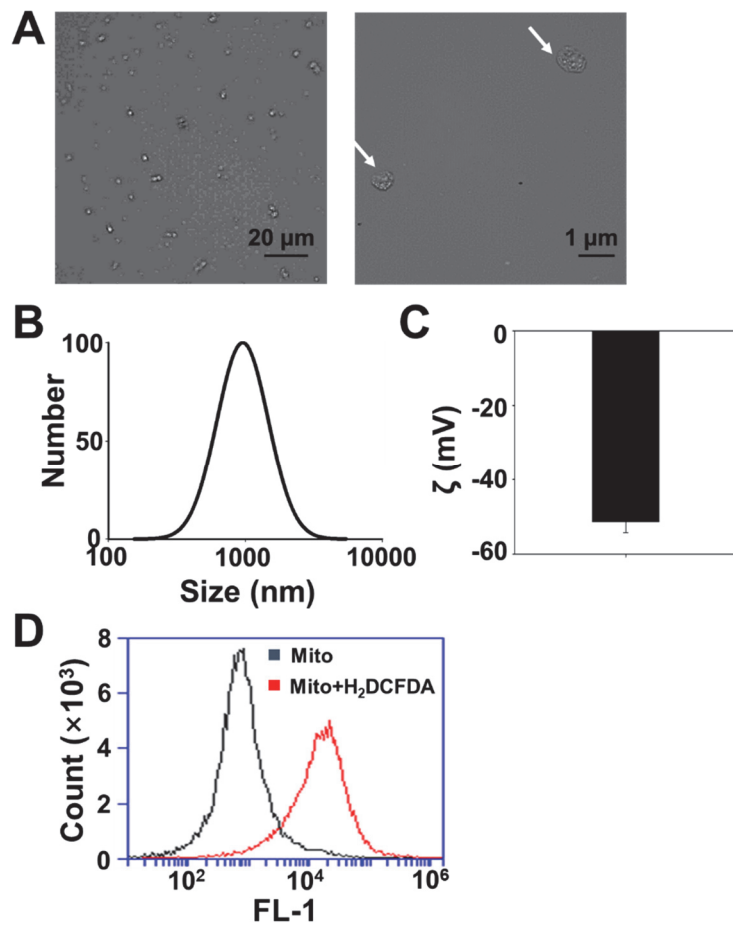


Fig. S21 Binding of the fluorescent materials with the isolated mitochondria. The isolated mitochondria were incubated with the fluorescein isothiocyanate (FITC), FITC-PEG2k-F7, or Rh123 in PBS for 1 h. After washing by PBS, the mitochondria were observed on a fluorescence microscope.

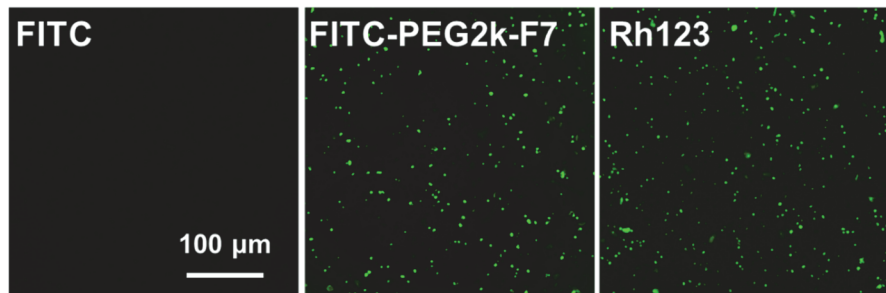


Fig. S22 Characterization of the liposomes. Mean particle size (A) and zeta potential (B) of the liposomes formulated by different phospholipids. Mean particle size (C) and zeta potential (D) of the cardiolipin-containing liposomes. The cardiolipin content was indicated. Data were expressed as the mean \pm SD.

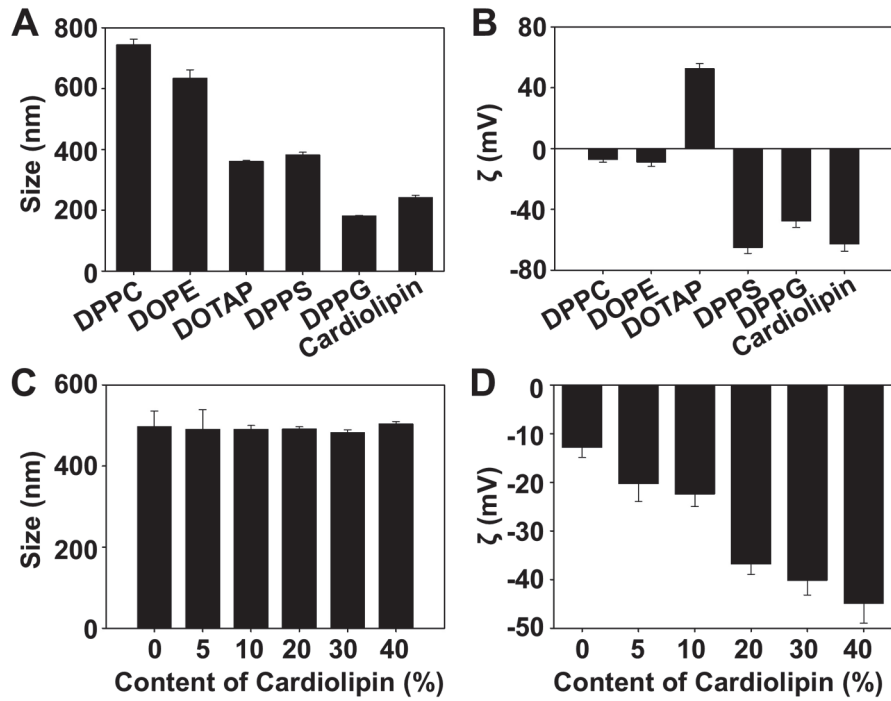


Fig. S23 Binding affinity of the fluorescent polymers or dyes with the natural phospholipids, determined by flow cytometry. Incubation time: 1 h.

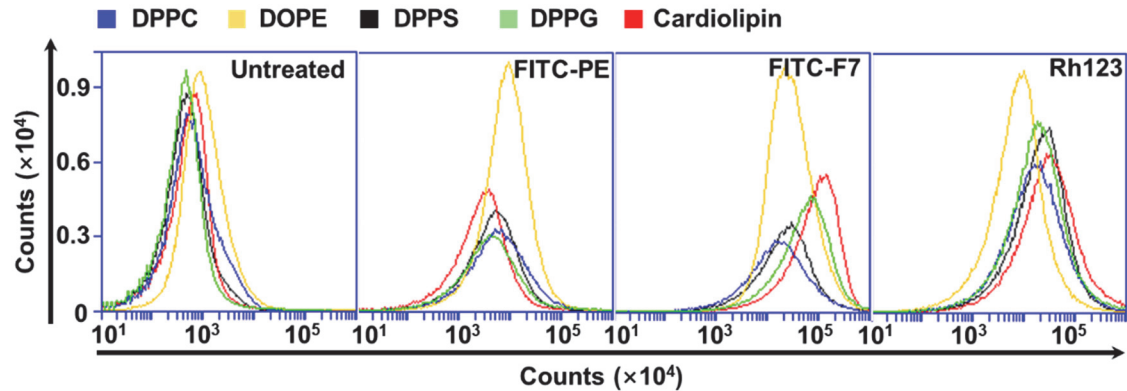


Fig. S24 Binding affinity of the FITC-F7 or FITC-PE with the cardiolipin-containing liposomes. The cardiolipin content was indicated. Incubation time: 1 h. MFI, mean fluorescence intensity. Data were expressed as the mean \pm SD.

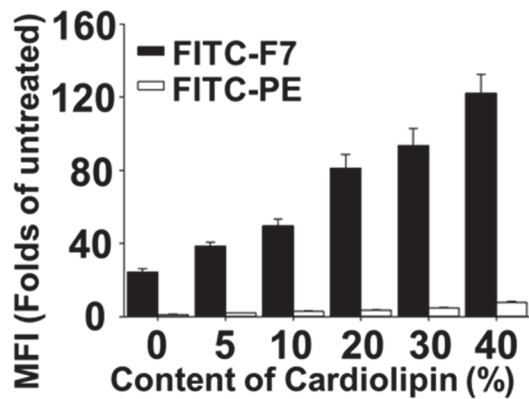


Fig. S25 Physicochemical characterization and drug release of the VES-loaded micelles. (A) Particle sizes of the VES-loaded micelles (pH 7.4) determined by dynamic light scattering (DLS). (B) Zeta potentials of the VES-loaded micelles (pH 7.4). (C) *In vitro* drug release determined by a widely used dialysis method⁹⁻¹¹. Note: Triphenylphosphonium (TPP) is a positively charged mitochondrial targeting ligand. Data were expressed as the mean \pm SD.

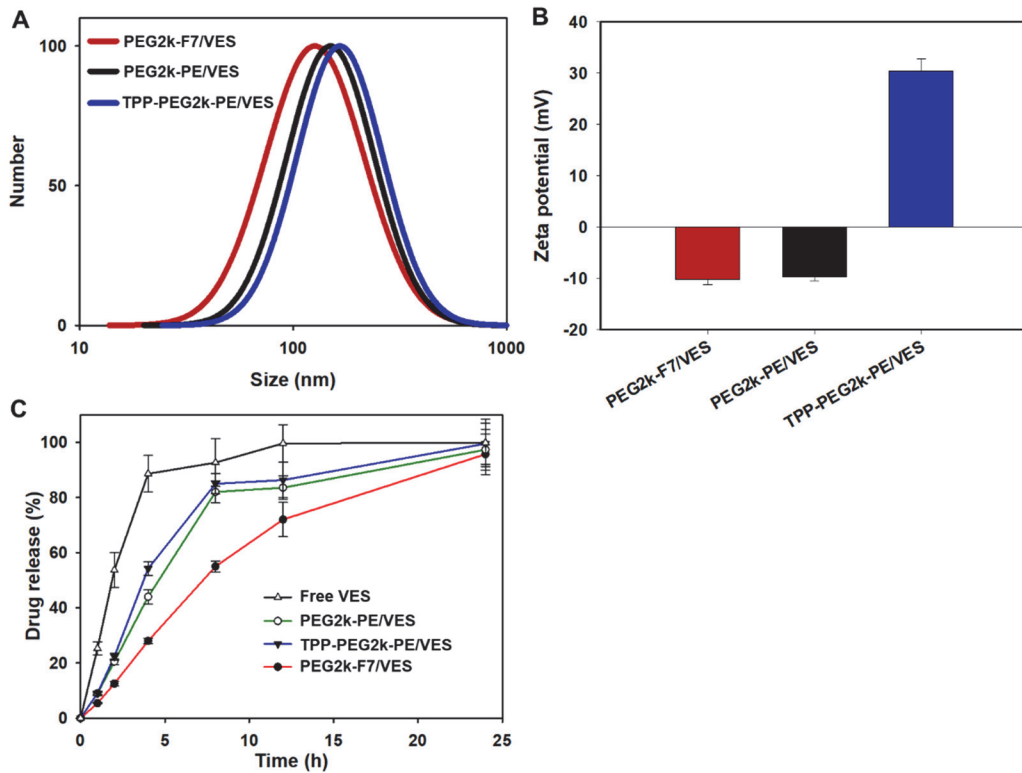


Fig. S26 Cytotoxicity of the VES-loaded micelles (A) and free polymers (B), determined by the CellTiter-Blue® Cell Viability assay. Incubation time: 48 h. (C) Mitochondrial Complex II activity assay. Incubation time: 1 h, VES dose: $50 \mu\text{g}\cdot\text{mL}^{-1}$. The free VES was dissolved in 0.1% DMSO. 2-Thenoyltrifluoroacetone (TTFA, 1 mM) was used as a positive control. Data were expressed as the mean \pm SD, * $p < 0.05$; *** $p < 0.001$.

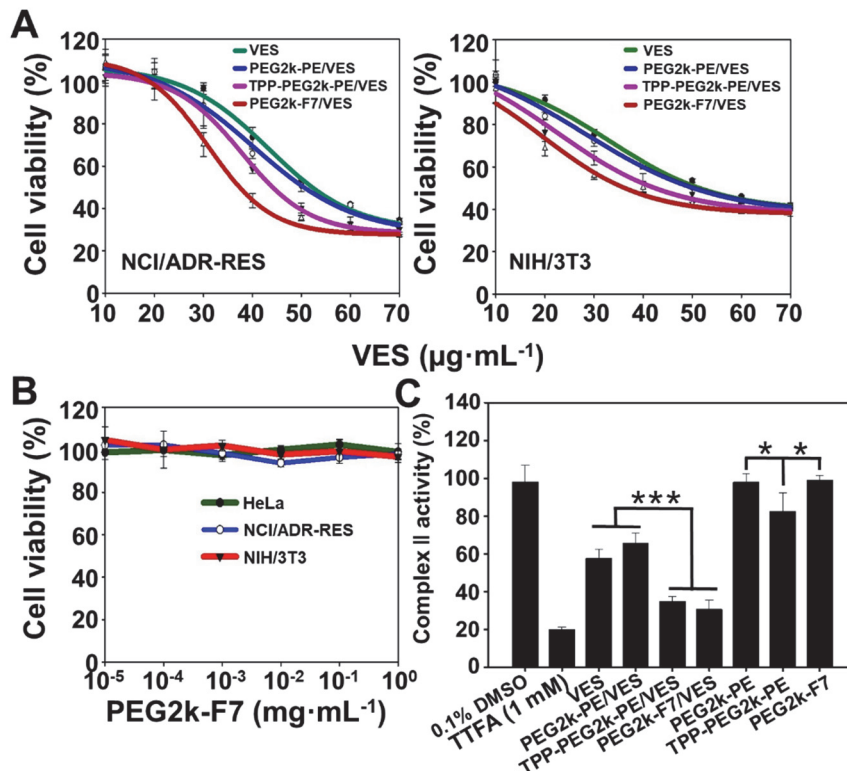


Fig. S27 Biodistribution of the Rh-PE (A), PEG2k-PE/Rh-PE (B), and PEG2k-F7/Rh-PE (C) at 2, 8, and 24 h. Animal model: 4T1-bearing BALB/c mice. Administration: single *i.v.* injection through the mouse tail vein. Data were expressed as the mean \pm SD.

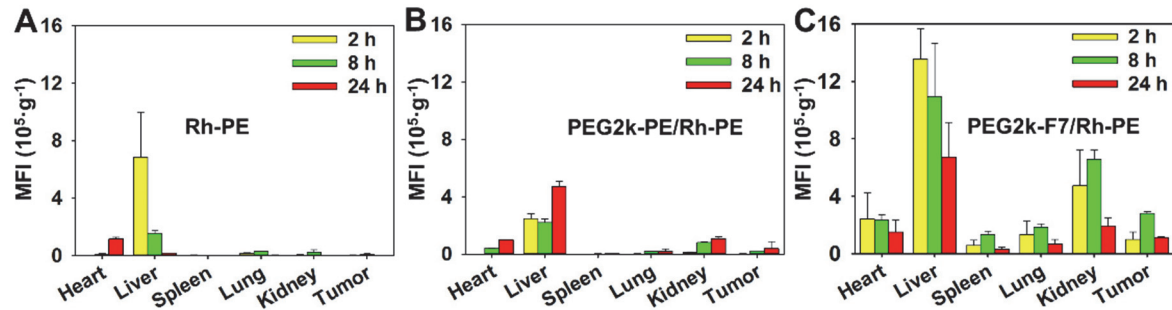
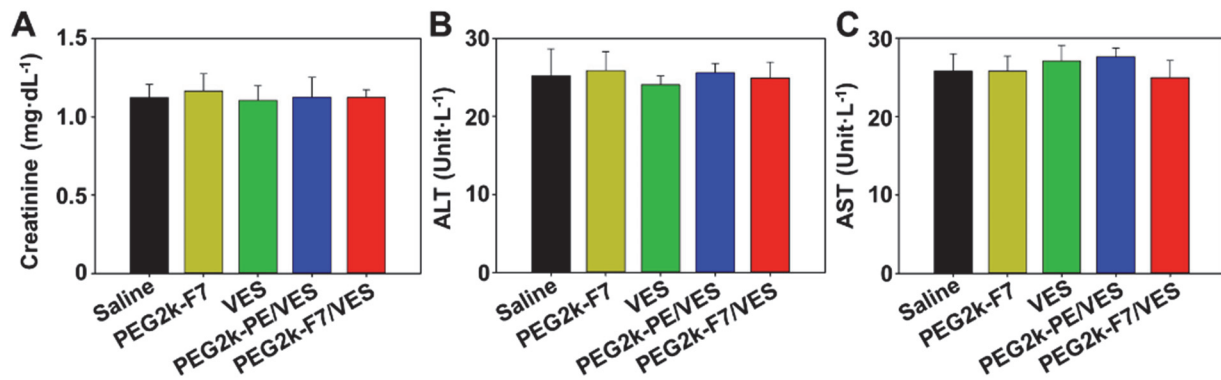


Fig. S28 Levels of the serum creatinine (A), alanine aminotransferase (ALT) (B), and aspartate aminotransferase (AST) (C). Animal model: 4T1-bearing BALB/c mice. Administration: *i.v.* injection through the mouse tail vein at $20 \text{ mg}\cdot\text{Kg}^{-1}$ VES every 4 days for three times. Data were expressed as the mean \pm SD.



Supporting videos

Video S1. Intracellular localization of the Rh-PE-labeled PEG2k-F7 micelles in the mitochondria, ER, and Golgi apparatus.

SI References

1. Zhu, L.; Kate, P.; Torchilin, V. P., Matrix Metalloprotease 2-Responsive Multifunctional Liposomal Nanocarrier for Enhanced Tumor Targeting. *ACS nano* **2012**, *6* (4), 3491-3498.
2. Dai, Z.; Yao, Q.; Zhu, L., MMP2-Sensitive PEG–Lipid Copolymers: A New Type of Tumor-Targeted P-Glycoprotein Inhibitor. *ACS applied materials & interfaces* **2016**, *8* (20), 12661-12673.
3. Fariss, M. W.; Merson, M. H.; O'Hara, T. M., A-Tocopheryl Succinate Protects Hepatocytes from Chemical-Induced Toxicity under Physiological Calcium Conditions. *Toxicol. Lett.* **1989**, *47* (1), 61-75.
4. Weber, T.; Lu, M.; Andera, L.; Lahm, H.; Gellert, N.; Fariss, M. W.; Korinek, V.; Sattler, W.; Ucker, D. S.; Terman, A., Vitamin E Succinate Is a Potent Novel Antineoplastic Agent with High Selectivity and Cooperativity with Tumor Necrosis Factor-Related Apoptosis-Inducing Ligand (Apo2 Ligand) *in Vivo*. *Clin. Cancer Res.* **2002**, *8* (3), 863-869.
5. Lu, J.; Owen, S. C.; Shoichet, M. S., Stability of Self-Assembled Polymeric Micelles in Serum. *Macromolecules* **2011**, *44* (15), 6002-6008.
6. Hayakawa, K.; Esposito, E.; Wang, X.; Terasaki, Y.; Liu, Y.; Xing, C.; Ji, X.; Lo, E. H., Transfer of Mitochondria from Astrocytes to Neurons after Stroke. *Nature* **2016**, *535* (7613), 551-555.
7. Temmerman, K.; Nickel, W., A Novel Flow Cytometric Assay to Quantify Interactions between Proteins and Membrane Lipids. *J. Lipid Res.* **2009**, *50* (6), 1245-1254.
8. Van Meer, G.; Voelker, D. R.; Feigenson, G. W., Membrane Lipids: Where They Are and How They Behave. *Nature reviews Molecular cell biology* **2008**, *9* (2), 112-124.
9. Yao, Q.; Choi, J. H.; Dai, Z.; Wang, J.; Kim, D.; Tang, X.; Zhu, L., Improving Tumor Specificity and Anticancer Activity of Dasatinib by Dual-Targeted Polymeric Micelles. *ACS applied materials & interfaces* **2017**, *9* (42), 36642-36654.
10. Yao, Q.; Liu, Y.; Kou, L.; Tu, Y.; Tang, X.; Zhu, L., Tumor-Targeted Drug Delivery and Sensitization by MMP2-Responsive Polymeric Micelles. *Nanomedicine: Nanotechnology, Biology and Medicine* **2019**, *19*, 71-80.
11. Zhu, L.; Wang, T.; Perche, F.; Taigind, A.; Torchilin, V. P., Enhanced Anticancer Activity of Nanopreparation Containing an MMP2-Sensitive PEG-Drug Conjugate and Cell-Penetrating Moiety. *Proceedings of the National Academy of Sciences* **2013**, *110* (42), 17047-17052.
12. Wang, J.; Lee, J. S.; Kim, D.; Zhu, L., Exploration of Zinc Oxide Nanoparticles as a Multitarget and Multifunctional Anticancer Nanomedicine. *ACS applied materials & interfaces* **2017**, *9* (46), 39971-39984.
13. Liu, Y.; Dai, Z.; Wang, J.; Tu, Y.; Zhu, L., Folate-Targeted pH-Sensitive Bortezomib Conjugates for Cancer Treatment. *Chem. Commun. (Camb.)* **2019**, *55* (29), 4254-4257.
14. Pulaski, B. A.; Ostrand-Rosenberg, S., Mouse 4T1 Breast Tumor Model. *Curr. Protoc. Immunol.* **2001**, *20.2*. 1-20.2. 16.
15. Liu, Y.; Wang, J.; Zhang, J.; Marbach, S.; Xu, W.; Zhu, L., Targeting Tumor-Associated Macrophages by MMP2-Sensitive Apoptotic Body-Mimicking Nanoparticles. *ACS applied materials & interfaces* **2020**, *12* (47), 52402-52414.